cosmetics

MDPI

Article

Evaluation of Cacumen Platycladi Extract for Hair Loss Prevention: Mechanisms, Efficacy, and Clinical Application

Xue-Dong Bai [1], Yu-Chen Liu [1], Hong-Yun Zhao [1], Yi-Zhou Luo [1], Li-Jun Xu [1,2,*] and Feng Luo [1,*]

[1] R&D Center of Shanghai Huiwen Biotech Co., Ltd., No. 879 Ziping Road, Shanghai 201318, China; xuedong_bai21@hotmail.com (X.-D.B.); lyc98675@21wenda.com (Y.-C.L.); zhy80571@21wenda.com (H.-Y.Z.); luoyz@21wenda.com (Y.-Z.L.)

[2] School of Resources and Environmental Engineering, Shanghai Polytechnic University, No. 2360 Jinhai Road, Shanghai 201209, China

* Correspondence: xulj@sspu.edu.cn (L.-J.X.); luofeng@21wenda.com (F.L.); Tel.: +86-021-58574488 (F.L.)

Abstract

Hair loss is a prevalent condition with various causes, and effective treatments are in high demand. Cacumen Platycladi (*Platycladus orientalis* leaves), a traditional Chinese medicine, has been historically used to prevent hair loss. This study aimed to evaluate the efficacy and mechanisms of Cacumen Platycladi extract (CPE) in preventing hair loss. Using a gradient extraction method with 1,3-butanediol, ethanol, and water, bioactive compounds like quercitrin, myricetin, and myricitrin were enriched and identified via Liquid Chromatography–Mass Spectrometry (LC-MS). The results showed that CPE inhibited 5α-reductase activity, enhanced the antioxidant capacity of human dermal papilla cells (HDPCs), and upregulated the phosphoinositide 3-kinase (PI3K)/protein kinase B (Akt)/mammalian target of rapamycin (mTOR) pathway to promote vascular endothelial growth factor (VEGF) and collagen type XVII (COL17) expression. A 12-week clinical trial demonstrated that CPE significantly reduced hair loss and increased local hair density compared to placebo, with no adverse effects. These findings support the potential of CPE as a safe and effective natural alternative for hair loss prevention.

Keywords: Cacumen Platycladi; hair loss; HDPCs; clinical trial

1. Introduction

Hair loss is a disorder of hair regeneration caused by disruptions or atrophy in the hair follicle cycle [1]. Common types of non-scarring alopecia include androgenetic alopecia, telogen effluvium, and alopecia areata [2]. Hair loss significantly impacts patients' mental well-being, social engagement, and quality of life [3]. Hair growth results from the development and differentiation of hair follicles, which are composed of HDPCs and epithelial cells [4]. Dysfunction in this process results in hair loss due to an imbalance in the hair follicle cycle. Hair follicle and hair growth occur in four distinct phases: anagen, catagen, telogen, and exogen [5]. The transition between these phases is controlled by various growth-promoting or inhibitory factors. Androgenetic alopecia (AGA)-presenting as male-pattern hair loss (MPHL) in men and female-pattern hair loss (FPHL) in women-is the most prevalent hair-loss disorder [6]. Clinically, it is characterized by progressive hair thinning with follicular miniaturization and reduced hair density [7]. The etiology is multifactorial, with aberrant dihydrotestosterone (DHT)–androgen-receptor (AR) signaling in scalp follicles and heightened follicular sensitivity to DHT as central features; genetic

Academic Editor: Lucia Montenegro

Received: 24 November 2025
Revised: 25 December 2025
Accepted: 8 January 2026
Published: 26 January 2026

predisposition and psychological stress act as modifiers, and additional contributors—such as microinflammation and oxidative stress—have been implicated [8–11].

The PI3K/AKT/mTOR signaling axis is a central regulator of cell proliferation and cell-cycle progression, playing an essential role in HDPCs and throughout the hair cycle [12]. Class I PI3K converts PIP2 to PIP3 to initiate downstream signaling and interfaces with cellular energy metabolism [13]. AKT orchestrates cell-cycle progression, autophagy, and apoptosis [14]. mTOR forms two functionally distinct complexes: mTORC1, activated downstream of AKT and pivotal in autophagy regulation, and mTORC2, which can phosphorylate AKT [15]. Collectively, the PI3K/AKT/mTOR pathway supports the proliferation and metabolic activity of HDPCs, thereby helping sustain the anagen phase [16].

The use of plant extracts for preventing hair loss is gaining increasing attention due to their advantages of minimal side effects and broad targeting mechanisms [17]. Multiple herbal agents have been reported to mitigate hair loss through diverse mechanisms, including improving scalp microcirculation, suppressing dihydrotestosterone (DHT) signaling via 5α-reductase inhibition, aromatherapy-based approaches, and nutritional support; representative examples include Phyllanthus emblica and Aloe barbadensis [18]. Cacumen Platycladi, the dried young branches and leaves of *Platycladus orientalis*, is traditionally considered bitter and astringent in Chinese medicine, used to cool the blood, stop bleeding [19]. It is primarily promoting hair growth, and enhance hair pigmentation, often applied in treating premature graying of hair and bleeding disorders. Cacumen Platycladi contains various active components, including flavonoids, polyphenols, terpenoids, and tannins, which have been extensively studied for their anti-inflammatory, antioxidant, and hair loss prevention properties [20–23]. Beyond traditional medicinal use, Cacumen Platycladi has also been investigated as a cosmeceutical ingredient for hair and scalp care. A water extract has been shown to promote the proliferation and migration of dermal papilla cells (DPCs) and to accelerate hair growth in mice via Akt-related signaling, accompanied by upregulation of hair growth-associated factors, including VEGF [24]. In addition, 12-week topical administration of the extract has been evaluated and was associated with increased terminal hair density through ACK1 [25]. Beyond hair care, it is also included in topical botanical formulas investigated for inflammatory skin disorders [26]. Nevertheless, additional mechanistic investigations are required to elucidate its underlying molecular mechanisms.

This study developed a targeted enrichment process for the different active components of Cacumen Platycladi. Using LC-MS, the active compounds in the extracts were analyzed. The antioxidant capacity and its ability to inhibit 5α-reductase, a key enzyme implicated in androgenetic alopecia, were evaluated. Results demonstrated that the extract can promote VEGF expression through the PI3K/Akt/mTOR signaling pathway, thereby enhancing COL17 expression. Additionally, a 12-week randomized, double-blind human clinical trial was conducted to further validate its effectiveness in preventing hair loss.

2. Materials and Methods

2.1. Materials

Cacumen Platycladi dried leaves were obtained from Anguo Jufu Chinese Herbal Medicine Co., Ltd. (Baoding, Hebei, China). SPF-grade C57BL/6J mice (18–23 g) were provided by Shanghai Model Organisms Center, Inc. (Shanghai, China). The mice were housed and bred by Shanghai Model Organisms Center, Inc., fed with standard chow and drinking water. After acclimating for 5–7 days, the experimental procedures were initiated to obtain epididymis tissue. All animal study protocols were approved by the Shanghai Model Organisms Center, Inc. (SYXK (Shanghai) 2023-0005). HDPCs were provided by Shanghai Zhong Qiao Xin Zhou Biotechnology Co., Ltd. (Shanghai, China).

Key reagents and materials were as follows: anhydrous ethanol (Aladdin, Shanghai, China), methanol (Aladdin, Shanghai, China), ddH_2O (Aladdin, Shanghai, China), 1,3-butanediol (Aladdin, Shanghai, China), D101 macroporous resin (Shanghai Yuanye Bio-Technology Co., Ltd., Shanghai, China), formic acid (UHPLC grade; Aladdin, Shanghai, China), acetonitrile (UHPLC grade; Aladdin, Shanghai, China), Tris buffer (1 M, pH 7.4; Sangon Biotech, Shanghai, China), phosphate-buffered saline (PBS, pH 7.4; Sangon Biotech, Shanghai, China), phenylmethylsulfonyl fluoride (PMSF; Beyotime, Shanghai, China), dithiothreitol (DTT; Solarbio, Shanghai, China), glycerol (Aladdin, Shanghai, China), nicotinamide adenine dinucleotide phosphate (NADPH; MCE, Monmouth Junction, NJ, USA), testosterone (Aladdin, Shanghai, China), dutasteride (TCI, Shanghai, China), hydrogen peroxide (30%; Aladdin, Shanghai, China), fetal bovine serum (FBS; Gibco, Thermo Fisher Scientific, Waltham, MA, USA), Dulbecco's modified Eagle's medium (DMEM; high-glucose; Gibco, Thermo Fisher Scientific, Waltham, MA, USA), penicillin–streptomycin (Gibco, Thermo Fisher Scientific, Waltham, MA, USA), ascorbic acid (Aladdin, Shanghai, China), fibroblast growth factor (FGF; Gibco, Thermo Fisher Scientific, Waltham, MA, USA), Triton X-100 (0.1%; Biosharp, Shanghai, China), 2′,7′-dichlorodihydrofluorescein diacetate (DCFH-DA) fluorescent probe (Beyotime, Shanghai, China), bovine serum albumin (BSA; Sangon Biotech, Shanghai, China), and an enhanced chemiluminescence (ECL) kit (Beyotime, Shanghai, China).

Primary antibodies used were: anti-PI3K p85α (ab191606; Abcam, Waltham, MA, USA), anti-AKT1 + AKT2 + AKT3 (ab179463; Abcam, Waltham, MA, USA), anti-phospho-AKT1 (Ser473) + AKT2 (Ser474) + AKT3 (Ser472) (ab192623, Abcam, Waltham, MA, USA), anti-mTOR (ab134903; Abcam, Waltham, MA, USA), anti-VEGFA (ab46154; Abcam, Waltham, MA, USA), anti-collagen XVII (ab184996; Abcam, Waltham, MA, USA), and anti-GAPDH (ab9485; Abcam, Waltham, MA, USA). Secondary antibody and nuclear stain were goat anti-rabbit IgG H&L (Alexa Fluor® 488, ab150077; Abcam, Waltham, MA, USA) and 4′,6-diamidino-2-phenylindole (DAPI, ab104139; Abcam, Waltham, MA, USA), respectively.

2.2. Preparation and Characterization of CPE

CPE was prepared according to a previously reported method with minor optimizations [27]. The dried leaves of Cacumen Platycladi were crushed into a fine powder. A solid-to-liquid ratio of 1:40 was used, and 1,3-butanediol was added. The mixture was subjected to continuous extraction at 40 °C for 5 h and then filtered to obtain solution A. The extraction residue was subjected to a second extraction with 80% (*v*/*v*) ethanol at a solid-to-solvent ratio of 1:30 (*w*/*v*; g/mL) at 60 °C for 3 h, followed by filtration. The filtrate was concentrated under reduced pressure to remove ethanol. The residue was then extracted with 10 volumes of purified water at 90 °C for 1 h, followed by filtration. The filtrates from both extractions were pooled and subjected to column purification using D101 macroporous resin. The adsorption flow rate was maintained at 3 BV/h. After adsorption, the resin was washed with purified water until the effluent tested negative for polysaccharides. The column effluent and water wash were combined and concentrated under reduced pressure to a concentration equivalent to 2× (*w*/*v*) of the starting material to yield Solution B. The column was then eluted with 80% (*v*/*v*) ethanol until no flavonoid reaction was detected; the eluate was concentrated under reduced pressure to remove ethanol to afford Solution C. Finally, Solutions A, B, and C were mixed at a volume ratio (*v*/*v*) of 2:1:17 to obtain the test solution of the CPE.

2.3. LC-MS Component Analysis

500 µL test solution centrifuged at 13,000× *g* for 10 min; supernatant collected and refrigerated at 4 °C no more than 24 h. The experimental procedure was performed as described previously with the established method [28]. The chromatographic system was an UltiMate™ 3000 UHPLC (Thermo Fisher Scientific, Waltham, MA, USA) equipped with an Acclaim™ 120 C18 Columns (1.9 µm, 2.1 mm × 100 mm; Thermo Fisher Scientific, Waltham, MA, USA). Chromatography: 0.3 mL/min flow, 10 µL injection; mobile phase A (water +0.1% formic acid) and B (acetonitrile +0.1% formic acid) with gradient elution (Table 1). Mass spectrometric detection was performed using a Q Exactive™ (Thermo Fisher Scientific, Waltham, MA, USA) equipped with a heated electrospray ionization (HESI) source. MS: HESI ion source (310 °C/320 °C; sheath/aux gas 30/10 arbitrary units); spray voltage 3 kV (+)/2.8 kV (−); DDA (loop count 10), HCD energy 10/28/35 eV. Primary MS: 70–1050 m/z, res 70k, AGC 3×10^6, 200 ms. Secondary MS: res 17.5k, AGC 1×10^5, 50 ms.

Table 1. Gradient elution program.

Time (min)	Mobile Phase A (%)	Mobile Phase B (%)
0	90	10
10	0	100
15	0	100
17.1	90	10
20	90	10

2.4. DPPH Scavenging Assay

Experimental procedures followed a previously reported protocol [29]. The test solution was serially diluted with distilled water. An aliquot of 0.2 mL of the diluted sample was mixed with 2.0 mL of Tris buffer, followed by the addition of 2.0 mL of 0.2 mmol/L DPPH in anhydrous ethanol. For the blank control group, 0.2 mL of ddH_2O was used instead of the test sample. For the color control group, 2 mL of anhydrous ethanol replaced the DPPH solution. After mixing, the reaction was incubated at 25 °C in the dark for 20 min, and absorbance was recorded at 520 nm. The DPPH radical scavenging rate was calculated according to Equation (1).

$$\text{DPPH Radical Scavenging Rate} = \left(1 - \frac{A_{sample} - A_{color}}{A_{blank}}\right) \times 100\%, \quad (1)$$

where A_{sample} = Absorbance of the test sample; A_{color} = Absorbance of the color control group; A_{blank} = Absorbance of the blank control group.

2.5. 5α-Reductase Inhibition Assay

Mouse epididymis tissue was homogenized in a buffer solution at a 1:5 (w/v) ratio, containing 1 mol/L Tris-HCl, 1 mmol/L PMSF, 1 mmol/L DTT, and 10% glycerol (pH 5.5) using a pre-cooled homogenizer. The crude homogenate was sequentially centrifuged (3500× *g*, 10 min; 10,000× *g*, 60 min; 10,000× *g*, 30 min) at 4 °C, collecting the supernatant after each step. The final supernatant was collected as the crude 5α-reductase preparation and stored at −80 °C until use.

For the reaction, add 25 µL of 0.833 mM testosterone solution followed by 25 µL of 10 mM NADPH solution, 100 µL of the test solution at varying concentrations, 100 µL of 1 M Tris-HCl buffer, and 100 µL of 5α-reductase. The mixture was vortexed and incubated at 37 °C for 30 min in a water bath. After the reaction, 500 µL of methanol was added to each tube to terminate the reaction. The mixture was vortexed, then centrifuged at 12,000× *g* for 10 min at room temperature. After filtration through a 0.45 µm membrane,

the residual testosterone content was measured using HPLC. The positive control was 50 μM dutasteride, and blank and reaction controls were also set. The 5α-reductase inhibition rate was calculated using the following Equation (2).

$$5\alpha\text{-Reductase Inhibition Rate} = \frac{C_{sample} - C_{reaction}}{C_{blank} - C_{reaction}} \times 100\% \quad (2)$$

where C_{sample} = Peak area of testosterone measured in the test sample; $C_{reaction}$ = Peak area of testosterone measured in the reaction control group; C_{blank} = Peak area of testosterone measured in the blank control group.

2.6. Cell Culture

HDPCs were cultured in complete medium–DMEM (high-glucose) supplemented with 10% FBS and 1% penicillin–streptomycin (*v*/*v*)-in a CO_2 incubator at 37 °C, 5% CO_2, and 95% RH. A total of 500 μL of cell suspension (1.0×10^5 cells/mL) was seeded per well into 24-well plates and cultured for 24 h before subsequent assays.

2.7. Effect of CPE on H_2O_2-Induced Reactive Oxygen Species (ROS) Levels in HDPCs

HDPCs were pre-incubated with complete medium containing different concentrations of CPE for 2 h. Then, 200 μM H_2O_2 was added to each well, and the cells were incubated for 4 h. After incubation, the cells were washed twice with PBS to complete the oxidative stress damage model induction. Next, 500 μL of PBS-diluted DCFH-DA fluorescence probe (1:1000) was added, and the cells were incubated for an additional 20 min. The cells were washed three times with PBS, fluorescence intensity was measured with a microplate reader (EX 495 nm/EM 545 nm). Control and model groups were also included in the experiment.

2.8. Western Blot Analysis of HDPCs

Following the previously established method with modifications [30]. HDPCs were incubated with complete medium containing different concentrations of CPE for 24 h. A positive control group was set with 10 ng/mL FGF, and a blank group was treated with PBS. After treatment, the cells were washed twice with PBS for subsequent Western blot analysis, which was performed as described previously. Protein bands were detected by enhanced chemiluminescence (ECL) (ChemiScope 6100, CLINX, Shanghai, China). Band intensities were quantified using ImageJ software (version 1.54). GAPDH was used as the loading control.

2.9. Immunofluorescence Detection of HDPCs

HDPCs were incubated with complete medium containing different concentrations of the test sample for 24 h, with PBS as the blank control group. After treatment, the cells were washed twice with PBS. Following established experimental protocols [29], COL17 was detected by immunofluorescence using Anti-Collagen XVII antibody (1:100) and goat anti-rabbit IgG H&L (Alexa Fluor® 488) (1:500). The cells were then incubated with DAPI in the dark, mounted, and imaged under an inverted fluorescence microscope. Image analysis and quantification were performed using ImageJ software.

2.10. Participants

This clinical study is a 12-week, double-blind, randomized, placebo-controlled, and self-comparison trial designed to evaluate the hair loss prevention efficacy of the CPE obtained through the process described in this paper. We selected and recruited 70 volunteers aged 40–60 years from Shanghai, with hair lengths ranging from 5 to 40 cm and more than 10 hairs counted using the 60 s combing method. The participants were randomly assigned

into two groups. Participants were required not to use any hair loss prevention or hair growth products during the study and to maintain their normal daily habits. All study procedures complied with the World Medical Association (WMA) Declaration of Helsinki (1964) and its later revisions. This study was conducted June–September 2022 at an independent laboratory operated by Shanghai Huiwen Biotech Corp., Ltd. (Shanghai, China). The protocol was reviewed and approved by the Institutional Review Board of Shanghai Huiwen Biotech Corp., Ltd. (Protocol No. HUIWEN BIO_2203A001). All participants were fully informed about the study procedures, read and understood the content of the informed consent form, and voluntarily signed the consent form.

2.11. Exclusion Criteria for Participants

Participants will be excluded if they have [31]: undergone hair treatments (dyeing, perming) in the past month; used hair loss or growth products in the past 3 months; taken medications affecting hair growth in the past 6 months; are pregnant, breastfeeding, or planning pregnancy; have severe androgenic alopecia, alopecia areata, scarring alopecia, or other scalp/hair disorders; have sleep or mood disorders; have previously undergone hair transplantation; or do not comply with study procedures.

2.12. Clinical Trial Content

The test sample is a scalp serum. The serum consists of 8% CPE, 82.5% water, 2% glycerin, 5% 1,3-propanediol, 2% 95% ethanol, and 0.5% PE9010. In the control group, CPE is replaced with an equal amount of water, while the other components remain the same. After mixing the components, the solution is stirred for 10 min at 150 rpm using a homogenizer (PRIMIX), then aliquoted, weighed, and distributed to the participants for use.

Participants must not get a haircut within two weeks before follow-up visits, must not wash their hair within 48 ± 4 h prior to follow-up, and are prohibited from combing their hair on the day of the visit. Measurements will be taken on day 0, and after 4, 8, and 12 weeks of product use. First, participants will undergo the 60-s hair combing method to count and record the number of hair strands lost [32]. Then, the hair on the top of the participant's head will be combed symmetrically to the sides and kept smooth. At each visit, the hairstyle should be maintained as close as possible to the initial state. Full scalp photos will be taken. Hair density in the top region will be assessed using the 0–7 scale (Table 2) and recorded as an overall hair density value. A fixed area of at least 1.5 cm × 1.5 cm on the participant's scalp (preferably in the temporal–parietal region) was marked for hair trimming. The location was carefully identified to ensure consistency at each visit. Hair in the marked area was trimmed to a residual length of no more than 1 mm. Images of the trimmed area were captured using the Foto//Pro Derma Medical Systems (DermLite, Courage+Khazaka Electronic GmbH, Mathias-Brüggen-Str., Germany), and local hair count and density were analyzed using the accompanying PhotoMAX PRO 4.2 (DERMA MEDICAL) software [33]. During image collection, the operator ensured the participant was in a comfortable position. The camera lens was placed directly over the center of the trimmed area for close-up image capture, ensuring the lens was in full contact with the scalp and kept perpendicular. The clarity of the captured images was checked before proceeding.

Table 2. Global Hair Density Grading Scale.

Grade	Description
0	No hair; scalp fully exposed.
1	Extremely sparse; scalp clearly visible.

Table 2. *Cont.*

Grade	Description
2	Sparse; scalp readily visible.
3	Moderately sparse; scalp visible.
4	Moderate density; scalp partially visible.
5	Moderately dense; scalp minimally visible.
6	Dense; scalp faintly visible.
7	Very dense; scalp not visible.

2.13. Adverse Event Monitoring

Adverse events were monitored based on participants' reports of discomfort or symptoms during the study. At each follow-up visit, trained dermatologists conducted safety and tolerability assessments to evaluate symptoms such as scalp irritation, hair texture changes, skin itching, and allergic reactions. Participants were required to promptly report any discomfort to the researchers during the study.

2.14. Statistical Analysis

Western blot and immunofluorescence images were analyzed using ImageJ to measure intensity. Statistical analyses were conducted using SPSS 21.0. Data were reported as mean ± standard error of the mean (SEM), with statistical significance set at $\alpha = 0.05$. ANOVA was used to evaluate primary and secondary outcomes by assessing within-group and over-time changes.

3. Results

3.1. LC-MS Component Analysis of CPE

The extracted ion chromatograms (EIC) of the test sample in both positive and negative ion modes are shown in Figure 1. Compound Discoverer software (V3.2, Thermo Fisher Scientific, USA) was used to compare the data against multiple databases, including ChemSpider Plant Database, ChEBI, ChEMBL, Natural Products Database, Chinese Medicine Powder Database, OTC Chinese Medicine Database, and mzCloud Database. High-matching compounds with peak area ratios greater than 1% were retained and are listed in Table 2.

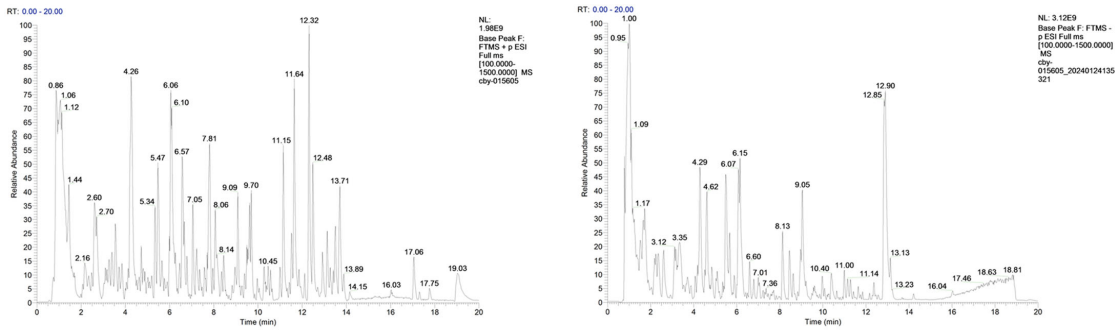

Figure 1. LC−MS Extracted Ion Chromatograms of CPE. After centrifugation, CPE was analyzed using LC−MS. Extracted ion chromatograms were obtained under positive ion mode (**a**) and negative ion mode (**b**) according to the mass spectrometry conditions.

The results indicate that the primary active components of the *Platycladus orientalis* extract are flavonoids, as shown in Table 3, with quercitrin, fisetin, myricetin, and myricitrin as the dominant compounds. Among these, quercitrin, myricitrin, and myricetin are identified as key active ingredients, which reduce oxidative stress damage to HDPCs,

stimulate follicular differentiation, and induce microvascular formation [21]. These findings provide a biochemical basis for the hair loss prevention efficacy of the CPE.

Table 3. LC-MS Analysis of CPE Components.

No.	Component	Molecular Formula	Retention Time (min)	Peak Area (%)
1	quercitrin	$C_{21}H_{20}O_{11}$	6.117	11.34395
2	Morin	$C_{15}H_{10}O_7$	6.059	8.34892
3	Myricitrin	$C_{21}H_{20}O_{12}$	5.492	7.99802
4	Choline	$C_5H_{13}NO$	0.923	5.93866
5	Tryptophan	$C_{11}H_{12}N_2O_2$	2.609	5.55619
6	Myricetin	$C_{15}H_{10}O_8$	5.475	4.05429
7	Retusin 7-Methyl Ether	$C_{17}H_{14}O_5$	12.484	3.78179
8	Kaempferol	$C_{15}H_{10}O_6$	5.693	3.32815
9	Pyrocatechuic Acid	$C_7H_6O_4$	2.185	3.04212
10	DL-Malic acid	$C_4H_6O_5$	1.922	2.54115
11	Quinic acid	$C_7H_{12}O_6$	0.787	2.52662
12	L-Phenylalanine	$C_9H_{11}NO_2$	1.499	1.71521
13	Kojic acid	$C_6H_6O_4$	1.475	1.54325
14	Avicularin	$C_{20}H_{18}O_{11}$	5.994	1.53772
15	Abietic Acid	$C_{20}H_{30}O_2$	11.853	1.50084
16	Cupressuflavone	$C_{30}H_{18}O_{10}$	8.961	1.44682
17	Aloenin	$C_{19}H_{22}O_{10}$	6.193	1.37251
18	(15Z)-9,12,13-Trihydroxy-15-octadecenoic acid	$C_{18}H_{34}O_5$	8.621	1.33715
19	Corchorifatty acid F	$C_{18}H_{32}O_5$	8.165	1.22631
20	5-Hydroxymethylfurfural	$C_6H_6O_3$	2.312	1.01082

3.2. Protective Effect of CPE on Oxidative Stress-Induced Damage in HDPCs

CPE was tested at final concentrations of 1.95 mg/mL to 62.5 mg/mL. The experimental results showed a clear dose-dependent relationship, with the DPPH scavenging rate significantly increasing as the concentration of CPE increased. IC50 is one of the key indicators used to measure the antioxidant activity of a substance, representing the concentration required to achieve 50% radical scavenging [34]. The data were fitted using the [Agonist] vs. response–Variable slope (four parameters) model, yielding an IC50 value of 8.31 mg/mL. The fitted curve is shown in Figure 2a.

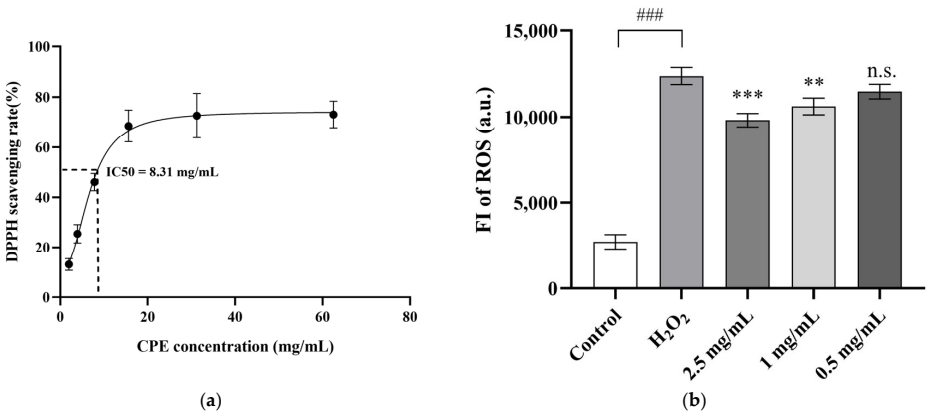

Figure 2. Protective Effect of CPE Against Oxidative Stress Damage in HDPCs. (**a**) The scavenging rate of DPPH free radicals by different concentrations of CPE was measured, and IC50 was obtained through nonlinear fitting. The concentration corresponding 50% scavenging rate point was indicated by dotted lines. (**b**) HDPCs were pretreated with CPE, followed by the induction of an oxidative stress damage model using H_2O_2. Intracellular ROS levels were detected using the DCFH-DA probe. Each group included three replicates, and the results are expressed as mean ± SEM. ### indicates a significant difference between the H_2O_2 and control groups ($p < 0.001$, one-way ANOVA). The differences between the CPE and control groups were analyzed by ANOVA: ** $p < 0.01$, *** $p < 0.001$, and n.s. $p > 0.05$.

CPE at final concentrations of 2.5 mg/mL and 1 mg/mL significantly reduced intracellular ROS levels in HDPCs by 20.7% ($p < 0.001$) and 14.3% ($p < 0.01$), respectively, as shown in Figure 2b. This indicates that CPE has a protective effect against endogenous oxidative stress-induced damage in HDPCs, with a dose-dependent relationship. These findings demonstrate that CPE mitigates oxidative stress damage, thereby protecting hair follicles.

3.3. Inhibition of 5α-Reductase Activity by CPE

The positive control, dutasteride, a known competitive inhibitor of 5α-reductase, demonstrated an inhibition rate of 81.25%, indicating the successful establishment of the in vitro 5α-reductase inhibition model. CPE was tested at final concentrations of 200 mg/mL, 60 mg/mL, 20 mg/mL, 6 mg/mL, 2 mg/mL, 0.6 mg/mL, and 0.2 mg/mL. As the concentration of CPE increased, its inhibition of 5α-reductase activity showed a clear dose-dependent effect. Data were analyzed by nonlinear fitting using the [Inhibitor] vs. normalized response—Variable slope model, yielding an IC50 value of 18.07 mg/mL. The fitted curve is shown in Figure 3.

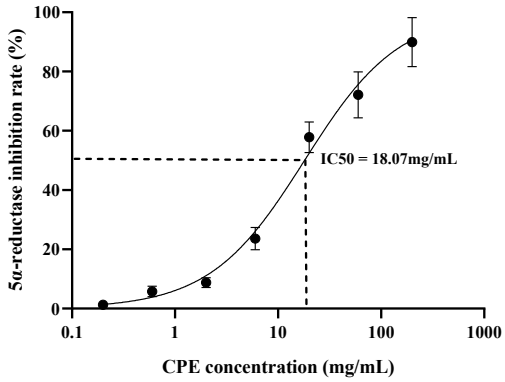

Figure 3. Inhibitory effect of CPE on 5α-reductase activity. Testosterone remaining in the reaction system at different concentrations of CPE was quantified by HPLC. The IC50 value was calculated using nonlinear regression analysis. The concentration corresponding 50% inhibition rate point was indicated by dotted lines. Each group included three replicates, and the results are presented as mean ± standard error of the mean (SEM).

3.4. CPE Promotes VEGF and COL17 Expression by HDPCs via the PI3K/Akt Signaling Pathway

The PI3K/Akt signaling pathway regulates the expression of VEGF, a growth factor that stimulates angiogenesis around hair follicles, improving follicular nutrition and regulating the hair follicle growth cycle [35,36]. COL17 is a transmembrane protein located between the epidermis and dermis, playing a crucial role in regulating basement membrane adhesion, skin aging mechanisms, and the maintenance of hair follicle stem cells, decrease in its levels is considered a signal of hair follicle stem cell aging [37–39].

Western blot results (Figure 4a) showed that compared with the blank control, CPE at concentrations of 5 mg/mL and 1 mg/mL upregulated the ratio of p-PI3K (Figure 4b) and p-Akt (Figure 4c) in HDPCs, promoted the phosphorylation of PI3K and Akt, and enhanced the expression of mTOR (Figure 4d), VEGF-A (Figure 4e), and COL17 (Figure 4g). These effects were observed in a dose-dependent manner.

Immunofluorescence results (Figure 4f) demonstrated that, compared to the control group, CPE at concentrations of 5 mg/mL and 1 mg/mL significantly promoted COL17 expression in HDPCs, with promotion rates of 98.25% ($p < 0.001$) and 39.64% ($p < 0.01$), respectively. This indicates that CPE promotes COL17 expression in HDPCs in a dose-dependent manner (Figure 4h).

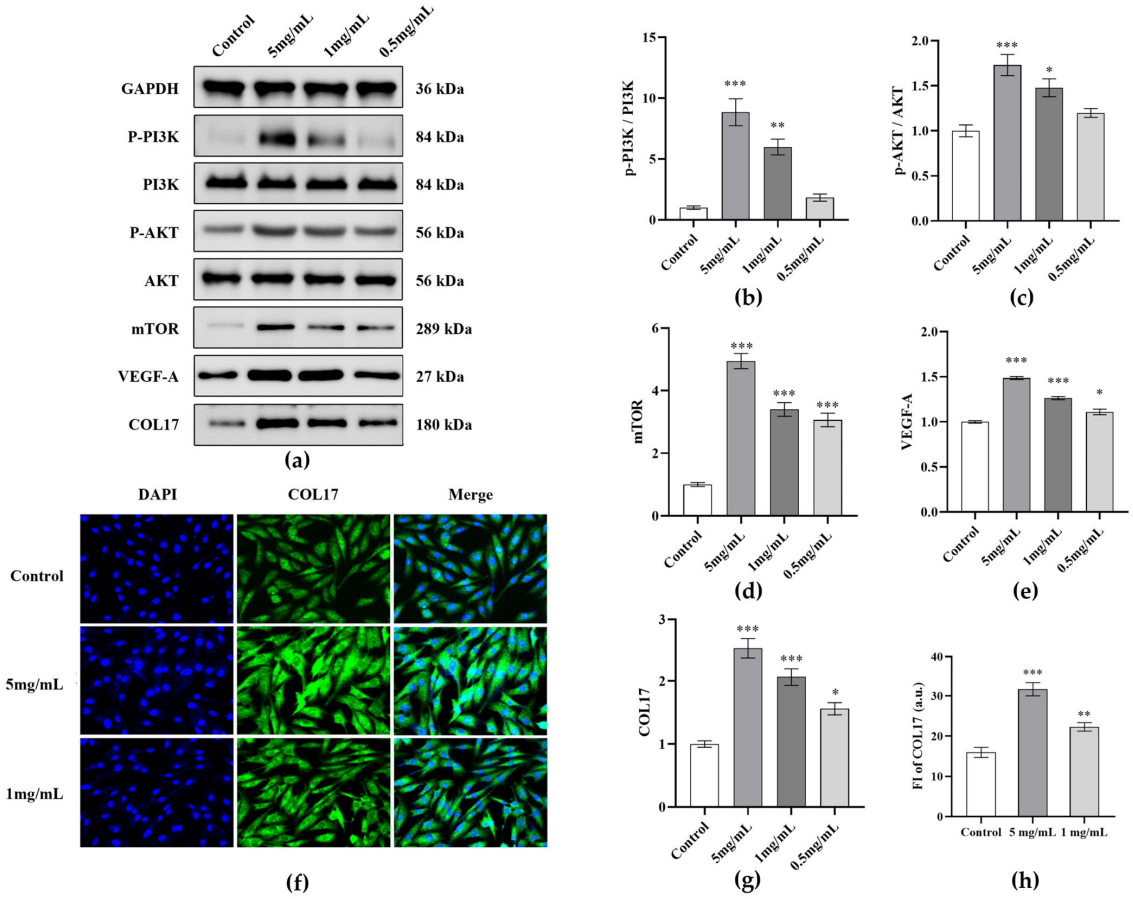

Figure 4. Analysis of CPE effects on protein expression in HDPCs. (**a**) Western blot imaging of protein expression after treating HDPCs with different concentrations of CPE for 24 h. Quantitative analysis of (**b**) p-PI3K/PI3K ratio, (**c**) p-AKT/AKT ratio, (**d**) mTOR, (**e**) VEGF-A, and (**g**) COL17 expression levels. (**f**) Immunofluorescence detection of COL17 expression in HDPCs: nuclei were stained with DAPI (blue), and COL17 was labeled with Alexa Fluor® 488 (green), scale bar = 100.00 µm. (**h**) Fluorescence intensity quantification and statistics were performed using ImageJ. Data are presented as mean ± SEM, the differences between the CPE and control groups were analyzed by ANOVA: * $p < 0.05$, ** $p < 0.01$, *** $p < 0.001$.

3.5. Clinical Trial of CPE for Hair Loss Prevention

Sixty volunteers were randomized into two equal groups of 30. The trial completion rates were 26 of 30 in the placebo group and 25 of 30 in the CPE group, with all dropouts attributed to personal reasons. No adverse reactions were reported by any participants. Participant information and baseline data are shown in Table 4.

Table 4. Participant information and baseline data.

Parameter		Placebo	CPE
Allocated Numbers		30	30
Drop Numbers		4	5
Analysis Numbers		26	25
Age (Years)		40.35 ± 8.77 [1]	41.48 ± 8.25 [1]
Sex	Female	19	21
	Male	7	4
Hair loss count		29.19 ± 2.51 [2]	40.04 ± 1.15 [2]
Overall hair density		4.90 ± 0.14 [2]	4.18 ± 0.15 [2]
Local hair density		166.78 ± 5.20 [2]	143.51 ± 4.89 [2]

[1] Statistical data is presented as Mean ± SD. [2] Statistical data is presented as Mean ± SEM.

The number of hairs lost during 60-s hair combing test, overall hair density, local hair density, and the difference in these measurements (Figure 5a–c) were statistically analyzed. The results showed that, compared to baseline values, the CPE group had a significant decrease in hair loss count after 4 weeks of product use ($p < 0.01$). After 8 weeks, hair loss count decreased significantly ($p < 0.001$), and the difference in local hair density was significantly higher than that of the placebo group ($p < 0.05$). After 12 weeks of product use, both hair loss count and local hair density significantly decreased ($p < 0.001$), and the differences in hair loss count and local hair density were both significantly higher than those of the placebo group ($p < 0.05$). Although there was no significant change in overall hair density compared to baseline values, the average score showed an upward trend, and after 12 weeks, 76% of the participants in the CPE group had an improved score. Representative case studies of participants were also presented, including hair loss count (Figure 5e), local hair density images (Figure 5d), and overall hair density collection cases (Figure 5f). Additional clinical case images are provided in Figure S1.

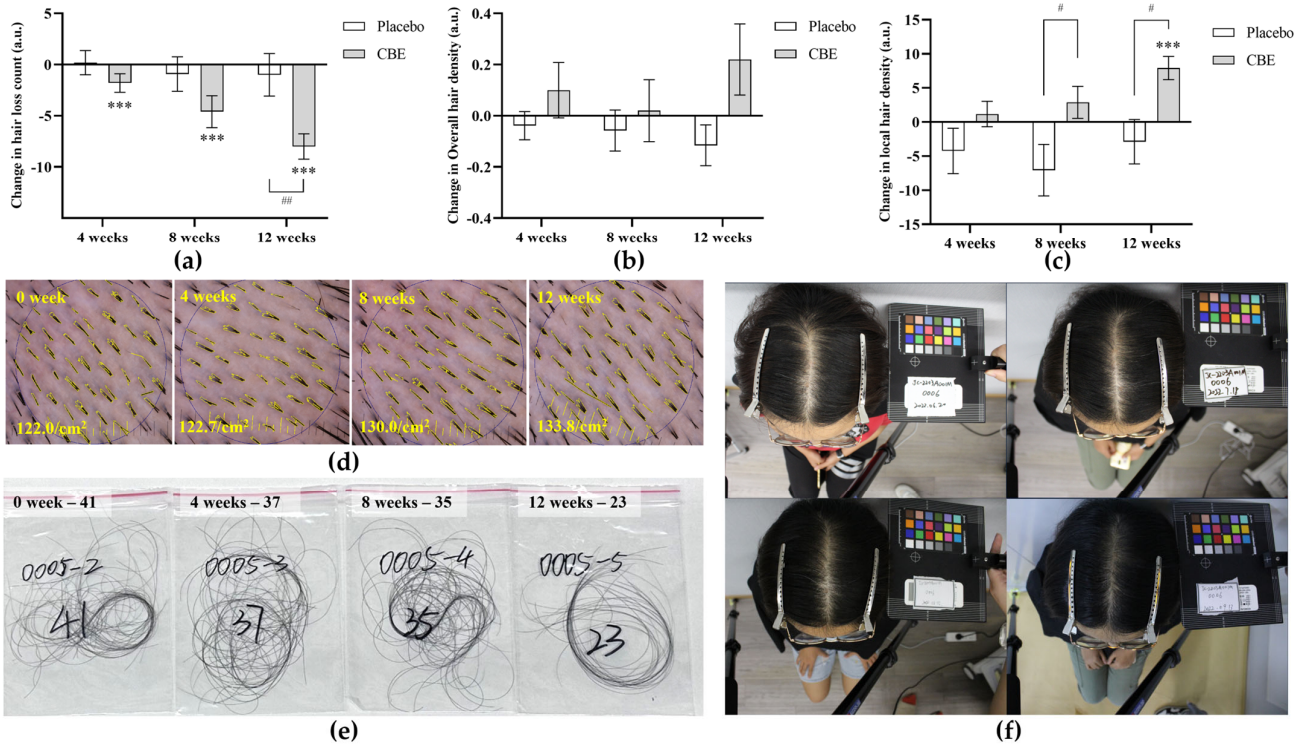

Figure 5. Clinical Trial Results of CPE for Hair Loss Prevention. Two groups of participants used either the CPE serum or the placebo serum for 12 weeks. The number of hairs lost during 60-s hair combing test (**a**), overall hair density (**b**), and local hair density (**c**) were measured. Data are presented as mean ± SEM. Between-group differences for the CPE and placebo groups were analyzed using a two-way ANOVA, with # indicating $p < 0.05$ and ## indicating $p < 0.01$. Within-group differences were analyzed using a paired *t*-test, with *** indicating $p < 0.001$. Representative case studies of participants include local hair density (**d**), hair loss count (**e**), and overall hair density (**f**).

4. Discussion

This study presents an extraction method for Cacumen Platycladi using a 1,3-butanediol, ethanol, and water gradient, which allows the selective enrichment of components with varying polarities. LC-MS analysis revealed that the main active components in the CPE are quercitrin, myricetin, and myricitrin. The mechanisms underlying its anti-hair loss effects include inhibiting 5α-reductase activity to reduce dihydrotestosterone-induced damage to hair follicles, enhancing HDPCs' resistance to oxidative stress, and upregulating PI3K/Akt/mTOR in HDPCs to promote the expression of VEGF and COL17. The results of

this study successfully demonstrate the effectiveness of the extraction method and further validate its multi-targeted mechanism of action in hair loss prevention. Furthermore, a 12-week human clinical trial confirmed its effectiveness and safety for preventing hair loss.

HDPCs play a crucial role in various types of hair loss and are closely associated with the hair follicle growth cycle and health. The CPE obtained through this process was analyzed by LC-MS and found to primarily consist of flavonoids. Quercitrin has been shown to directly stimulate HDPCs by enhancing mitochondrial energy metabolism and MAPK/CREB signaling pathway [40]. The physiological activities of myricetin and myricetin that promote hair growth include antioxidant activity [41]. HDPC function under oxidative or stress conditions relevant to hair loss. DCFH-DA is a cell-permeable, non-fluorescent probe that, once inside the cell, is hydrolyzed by intracellular esterases to produce DCFH. DCFH cannot cross the cell membrane and is oxidized by intracellular ROS to generate DCF, which exhibits green fluorescence. The fluorescence intensity of DCF reflects the intracellular ROS levels. Thianthanyakij et al. reported that HDPCs are highly sensitive to oxidative stress, which can induce tissue hypoxia and follicular ischemia, leading to follicular atrophy and degradation [42,43].

Reported 5α-reductase inhibitors include FDA-approved drugs like finasteride [44] and dutasteride [45], as well as natural flavonoids and polyphenols from plant extracts, such as myricitrin, myricetin, quercetin, and kaempferol [42]. The CPE obtained through this process contains these compounds in high proportions, which may serve as the biochemical basis for its 5α-reductase inhibitory activity. The upregulation of the PI3K/Akt/mTOR pathway promotes VEGF expression, which enhances perifollicular angiogenesis, resulting in increased size of hair follicles and shafts [46]. To address potential concerns regarding cytotoxicity at higher doses and to verify that the concentrations showing activity in biochemical assays are physiologically achievable in cellular models, we additionally assessed the effects of CPE on HDPCs viability (Figure S2). The highest non-cytotoxic concentration of CPE in HDPCs was 10 mg/mL, which covered the concentrations used in our cellular assays and the DPPH IC50, but remained below the 5α-reductase IC50. This concentration window is consistent with a multi-pathway mode of action in HDPCs, in which antioxidant effects and PI3K/Akt/mTOR-associated signaling may represent major contributors, whereas 5α-reductase inhibition may play a secondary role. In our clinical trial, we aimed to objectively evaluate the efficacy of anti-hair loss cosmetics in preventing or reducing hair loss and maintaining or increasing hair count. By controlling various factors influencing hair loss, we selected reproducible and comparable quantitative indicators, such as hair loss count and hair density, before and after product use. The results demonstrated the clinical efficacy of CPE in preventing hair loss. Additionally, no adverse reactions were reported during the 12-week trial period, highlighting its favorable safety profile. In conclusion, Cacumen Platycladi extract obtained via a 1,3-butanediol–ethanol–water gradient shows multi-target anti-hair loss activity. Further work should strengthen translational development by establishing pathway dependency through pharmacological inhibition or genetic perturbation of the PI3K/Akt/mTOR axis in dermal papilla models, ideally complemented by ex vivo human hair follicle organ culture or in vivo alopecia models to link molecular changes with anagen maintenance and hair shaft outcomes. In parallel, network pharmacology integrating LC–MS–defined constituents with target prediction and pathway enrichment could be used to build a compound–target–pathway–phenotype network and prioritize key nodes for experimental validation. Collectively, these steps will clarify the clinical positioning of CPE and support its development as a botanical active for anti-hair loss formulations and as a complementary approach in hair-loss management.

Supplementary Materials: The following supporting information can be downloaded at: https://www.mdpi.com/article/10.3390/cosmetics13010028/s1, Figure S1: Supplementary clinical case images from the clinical trial evaluating CPE for hair loss prevention; Figure S2: Effects of CPE on the viability of HDPCs; Table S1: Components of CPE obtained by LC-MS analysis.

Author Contributions: Conceptualization, X.-D.B.; methodology, X.-D.B., Y.-C.L. and H.-Y.Z.; validation, X.-D.B. and H.-Y.Z.; formal analysis, X.-D.B. and Y.-C.L.; investigation, X.-D.B. and H.-Y.Z.; resources, L.-J.X.; data curation, X.-D.B. and Y.-C.L.; writing—original draft, X.-D.B.; writing—review and editing, L.-J.X.; visualization, X.-D.B. and Y.-C.L.; supervision, Y.-Z.L., L.-J.X. and F.L.; project administration, Y.-Z.L. and L.-J.X.; funding acquisition, F.L. All authors have read and agreed to the published version of the manuscript.

Funding: This research received no external funding.

Institutional Review Board Statement: The study was conducted in accordance with the Declaration of Helsinki, and approved by the Institutional Review Board of Shanghai Huiwen Biotech Corp., Ltd. (Protocol No. HUIWEN BIO_2203A001, 6 December 2022). The animal study protocol was approved by the Institutional Review Board of Shanghai Model Organisms Center, Inc. (SYXK (Shanghai) 2023-0005). The test product used in this study meets the National Medical Products Administration of China (NMPA) definition of a cosmetic. It was conducted in accordance with the Working Specifications for Cosmetics Registration and Filing Testing issued by the NMPA (official index number FGWJ-2020-1782). The institution that conducted this trial is a CMA-accredited testing institution in China, and its qualifications and capability scope have been reviewed and approved by the NMPA as meeting the above regulatory requirements. Therefore, ethical approval by the institution's internal ethics committee is sufficient for this type of cosmetic clinical trial, and the approval number is issued as an internal reference number.

Informed Consent Statement: Informed consent was obtained from all participants involved in the study. Written informed consent has been obtained from the patients to publish this paper.

Data Availability Statement: The data presented in this study are available on request from the corresponding author due to privacy and ethical reasons.

Acknowledgments: This work was supported by the Shanghai Huiwen Biotech Corp., Ltd., Shanghai, China.

Conflicts of Interest: X.-D.B., Y.-C.L., H.-Y.Z., Y.-Z.L., L.-J.X. and F.L. are employed by R&D Center of Shanghai Huiwen Biotech Co., Ltd., China. The funders had no role in the design of the study; in the collection, analyses or interpretation of data; in the writing of the manuscript; or in the decision to publish the results.

References

1. Oh, J.W.; Kloepper, J.; Langan, E.A.; Kim, Y.; Yeo, J.; Kim, M.J.; Hsi, T.C.; Rose, C.; Yoon, G.S.; Lee, S.J.; et al. A Guide to Studying Human Hair Follicle Cycling In Vivo. *J. Investig. Dermatol.* **2016**, *136*, 34–44. [CrossRef] [PubMed]
2. Schneider, M.R.; Schmidt-Ullrich, R.; Paus, R. The hair follicle as a dynamic miniorgan. *Curr. Biol.* **2009**, *19*, R132–R142. [CrossRef] [PubMed]
3. Huang, C.H.; Fu, Y.; Chi, C.C. Health-Related Quality of Life, Depression, and Self-esteem in Patients with Androgenetic Alopecia: A Systematic Review and Meta-analysis. *JAMA Dermatol.* **2021**, *157*, 963–970. [CrossRef]
4. Zhang, Y.; Huang, J.; Fu, D.; Liu, Z.; Wang, H.; Wang, J.; Qu, Q.; Li, K.; Fan, Z.; Hu, Z.; et al. Transcriptome Analysis Reveals an Inhibitory Effect of Dihydrotestosterone-Treated 2D- and 3D-Cultured Dermal Papilla Cells on Hair Follicle Growth. *Front. Cell Dev. Biol.* **2021**, *9*, 724310. [CrossRef]
5. Natarelli, N.; Gahoonia, N.; Sivamani, R.K. Integrative and Mechanistic Approach to the Hair Growth Cycle and Hair Loss. *J. Clin. Med.* **2023**, *12*, 893. [CrossRef]
6. Correa, A.C.; Machado, C.J.; Carneiro, S.C.S. Split-scalp pilot study to evaluate effectiveness of Minoxidil 0,5% MMP(R) versus Topical Minoxidil 5% in the treatment of Female Pattern Hair Loss. *Arch. Dermatol. Res.* **2024**, *316*, 313. [CrossRef]
7. Alessandrini, A.; Bruni, F.; Piraccini, B.M.; Starace, M. Common causes of hair loss–clinical manifestations, trichoscopy and therapy. *J. Eur. Acad. Dermatol. Venereol.* **2021**, *35*, 629–640. [CrossRef]

8. Zheng, M.; An, S.; Park, I.G.; Kim, J.; Kim, W.S.; Noh, M.; Sung, J.H. Differential Expression of CXCL12 in Human and Mouse Hair: Androgens Induce CXCL12 in Human Dermal Papilla and Dermal Sheath Cup. *Int. J. Mol. Sci.* **2024**, *26*, 95. [CrossRef]
9. Chen, S.; Li, L.; Ding, W.; Zhu, Y.; Zhou, N. Androgenetic Alopecia: An Update on Pathogenesis and Pharmacological Treatment. *Drug Des. Dev. Ther.* **2025**, *19*, 7349–7363. [CrossRef]
10. Cuevas-Diaz Duran, R.; Martinez-Ledesma, E.; Garcia-Garcia, M.; Bajo Gauzin, D.; Sarro-Ramirez, A.; Gonzalez-Carrillo, C.; Rodriguez-Sardin, D.; Fuentes, A.; Cardenas-Lopez, A. The Biology and Genomics of Human Hair Follicles: A Focus on Androgenetic Alopecia. *Int. J. Mol. Sci.* **2024**, *25*, 2542. [CrossRef]
11. Thom, E. Stress and the Hair Growth Cycle: Cortisol-Induced Hair Growth Disruption. *J. Drugs Dermatol. JDD* **2016**, *15*, 1001–1004.
12. Zhang, X.; Zhou, D.; Ma, T.; Liu, Q. Vascular Endothelial Growth Factor Protects CD200-Rich and CD34-Positive Hair Follicle Stem Cells Against Androgen-Induced Apoptosis Through the Phosphoinositide 3-Kinase/Akt Pathway in Patients with Androgenic Alopecia. *Dermatol. Surg.* **2020**, *46*, 358–368. [CrossRef] [PubMed]
13. Rathinaswamy, M.K.; Burke, J.E. Class I phosphoinositide 3-kinase (PI3K) regulatory subunits and their roles in signaling and disease. *Adv. Biol. Regul.* **2020**, *75*, 100657. [CrossRef] [PubMed]
14. Manning, B.D.; Toker, A. AKT/PKB signaling: Navigating the network. *Cell* **2017**, *169*, 381–405. [CrossRef]
15. Shorning, B.Y.; Dass, M.S.; Smalley, M.J.; Pearson, H.B. The PI3K-AKT-mTOR pathway and prostate cancer: At the crossroads of AR, MAPK, and WNT signaling. *Int. J. Mol. Sci.* **2020**, *21*, 4507. [CrossRef]
16. Chen, Y.; Fan, Z.; Wang, X.; Mo, M.; Zeng, S.B.; Xu, R.H.; Wang, X.; Wu, Y. PI3K/Akt signaling pathway is essential for de novo hair follicle regeneration. *Stem Cell Res. Ther.* **2020**, *11*, 144. [CrossRef]
17. Masoud, F.; Alamdari, H.A.; Asnaashari, S.; Shokri, J.; Javadzadeh, Y. Efficacy and safety of a novel herbal solution for the treatment of androgenetic alopecia and comparison with 5% minoxidil: A double-blind, randomized controlled trial study. *Dermatol. Ther.* **2020**, *33*, e14467. [CrossRef]
18. Elnady, R.E.; Abdon, M.S.; Shaheen, H.R.; Eladawy, R.M.; Azar, Y.O.; Al Raish, S.M. The Future of Alopecia Treatment: Plant Extracts, Nanocarriers, and 3D Bioprinting in Focus. *Pharmaceutics* **2025**, *17*, 584. [CrossRef]
19. Liu, G.; Cao, L. Chinese Herbal Medicine. In *Clinical Essentials of Contem-Porary Series of Chinese Medicine*; Huaxia Publishing House: Nanjing, China, 2000.
20. Darwish, R.S.; Hammoda, H.M.; Ghareeb, D.A.; Abdelhamid, A.S.; Harraz, F.M.; Shawky, E. Seasonal dynamics of the phenolic constituents of the cones and leaves of oriental Thuja (Platycladus orientalis L.) reveal their anti-inflammatory biomarkers. *RSC Adv.* **2021**, *11*, 24624–24635. [CrossRef]
21. Shan, M.; Li, S.F.Y.; Yu, S.; Qian, Y.; Guo, S.; Zhang, L.; Ding, A. Chemical Fingerprint and Quantitative Analysis for the Quality Evaluation of Platycladi cacumen by Ultra-performance Liquid Chromatography Coupled with Hierarchical Cluster Analysis. *J. Chromatogr. Sci.* **2018**, *56*, 41–48. [CrossRef]
22. Zhang, Y.; Han, L.; Chen, S.S.; Guan, J.; Qu, F.Z.; Zhao, Y.Q. Hair growth promoting activity of cedrol isolated from the leaves of Platycladus orientalis. *Biomed. Pharmacother.* **2016**, *83*, 641–647. [CrossRef]
23. Fan, S.Y.; Zeng, H.W.; Pei, Y.H.; Li, L.; Ye, J.; Pan, Y.X.; Zhang, J.G.; Yuan, X.; Zhang, W.D. The anti-inflammatory activities of an extract and compounds isolated from Platycladus orientalis (Linnaeus) Franco in vitro and ex vivo. *J. Ethnopharmacol.* **2012**, *141*, 647–652. [CrossRef] [PubMed]
24. Fu, H.; Li, W.; Weng, Z.; Huang, Z.; Liu, J.; Mao, Q.; Ding, B. Water extract of Cacumen platycladi promotes hair growth through the Akt/GSK3beta/beta-catenin signaling pathway. *Front. Pharmacol.* **2023**, *14*, 1038039. [CrossRef]
25. Kim, J.; Joo, J.H.; Kim, J.; Rim, H.; Shin, J.Y.; Choi, Y.H.; Min, K.; Lee, S.Y.; Jun, S.H.; Kang, N.G. Platycladus orientalis Leaf Extract Promotes Hair Growth via Non-Receptor Tyrosine Kinase ACK1 Activation. *Curr. Issues Mol. Biol.* **2024**, *46*, 11207–11219. [CrossRef] [PubMed]
26. Mechesso, A.F.; Lee, S.J.; Park, N.H.; Kim, J.Y.; Im, Z.E.; Suh, J.W.; Park, S.C. Preventive effects of a novel herbal mixture on atopic dermatitis-like skin lesions in BALB/C mice. *BMC Complement. Altern. Med.* **2019**, *19*, 25. [CrossRef]
27. Feng, L.; Yang, H.Y.; Ma, D.Y. Composition Containing Cacumen platycladi Extract and Its Preparation Method and Applications. China Patent CN109464317A, 15 March 2019. (In Chinese)
28. Zhou, J.; Gao, W.; Xie, L.; Zhang, R.; Zhang, Y.; Wei, Z. Revealing mechanism of phenol-amine reaction to form humus in compost based on high-resolution liquid chromatography mass spectrometry and spectroscopy. *Bioresour. Technol.* **2024**, *403*, 130862. [CrossRef]
29. Bai, X.D.; Fei, W.C.; Liu, Y.C.; Yang, S.P. Enzymatically modified isoquercitrin and its protective effects against photoaging: In-vitro and clinical studies. *Photochem. Photobiol.* **2024**, *100*, 1475–1488. [CrossRef]
30. Li, X.; Xie, X.; Zhang, L.; Meng, Y.; Li, N.; Wang, M.; Zhai, C.; Liu, Z.; Di, T.; Zhang, L. Hesperidin inhibits keratinocyte proliferation and imiquimod-induced psoriasis-like dermatitis via the IRS-1/ERK1/2 pathway. *Life Sci.* **2019**, *219*, 311–321. [CrossRef]
31. Nobile, V.; Cestone, E.; Roveda, G.; Pisati, M.; Michelotti, A.; Dossena, M. Double Blind, Randomized, Placebo-Controlled Assessment of the Efficacy of a Food Supplement in Reducing Hair Loss in Male Subjects. *J. Cosmetol.* **2021**, *7*, 171.

32. Wasko, C.A.; Mackley, C.L.; Sperling, L.C.; Mauger, D.; Miller, J.J. Standardizing the 60-second hair count. *Arch. Dermatol.* **2008**, *144*, 759–762. [CrossRef]
33. Chen, Q.; Tao, Q.; Zhu, Q.; Zhu, J.; Du, X. Association between trichoscopic features and serum hormone levels and vitamin D concentration in patients with androgenetic alopecia in Eastern China: A cross-sectional study. *Clin. Cosmet. Investig. Dermatol.* **2023**, *16*, 2547–2555. [CrossRef] [PubMed]
34. Cornea, A.C.; Marc, G.; Ionuț, I.; Moldovan, C.; Fizeșan, I.; Petru, A.E.; Creștin, I.V.; Pîrnău, A.; Vlase, L.; Oniga, O. Synthesis, Cytotoxicity and Antioxidant Activity Evaluation of Some Thiazolyl–Catechol Compounds. *Antioxidants* **2024**, *13*, 937. [CrossRef] [PubMed]
35. Karar, J.; Maity, A. PI3K/AKT/mTOR pathway in angiogenesis. *Front. Mol. Neurosci.* **2011**, *4*, 51. [CrossRef] [PubMed]
36. Yano, K.; Brown, L.F.; Detmar, M. Control of hair growth and follicle size by VEGF-mediated angiogenesis. *J. Clin. Investig.* **2001**, *107*, 409–417. [CrossRef]
37. Natsuga, K.; Watanabe, M.; Nishie, W.; Shimizu, H. Life before and beyond blistering: The role of collagen XVII in epidermal physiology. *Exp. Dermatol.* **2019**, *28*, 1135–1141. [CrossRef]
38. Liu, N.; Matsumura, H.; Kato, T.; Ichinose, S.; Takada, A.; Namiki, T.; Asakawa, K.; Morinaga, H.; Mohri, Y.; De Arcangelis, A. Stem cell competition orchestrates skin homeostasis and ageing. *Nature* **2019**, *568*, 344–350. [CrossRef]
39. Watanabe, M.; Natsuga, K.; Nishie, W.; Kobayashi, Y.; Donati, G.; Suzuki, S.; Fujimura, Y.; Tsukiyama, T.; Ujiie, H.; Shinkuma, S. Type XVII collagen coordinates proliferation in the interfollicular epidermis. *eLife* **2017**, *6*, e26635. [CrossRef]
40. Kim, J.; Kim, S.R.; Choi, Y.H.; Shin, J.Y.; Kim, C.D.; Kang, N.G.; Park, B.C.; Lee, S. Quercitrin stimulates hair growth with enhanced expression of growth factors via activation of MAPK/CREB signaling pathway. *Molecules* **2020**, *25*, 4004. [CrossRef]
41. Kang, N.J.; Jung, S.K.; Lee, K.W.; Lee, H.J. Myricetin is a potent chemopreventive phytochemical in skin carcinogenesis. *Ann. N. Y. Acad. Sci.* **2011**, *1229*, 124–132. [CrossRef]
42. Matsuda, H.; Yamazaki, M.; Matsuo, K.; Asanuma, Y.; Kubo, M. Anti-androgenic activity of Myricae Cortex—Isolation of active constituents from bark of Myrica rubra. *Biol. Pharm. Bull.* **2001**, *24*, 259–263. [CrossRef]
43. Thianthanyakij, T.; Zhou, Y.; Wu, M.; Zhang, Y.; Lin, J.M.; Huang, Y.; Sha, Y.; Wang, J.; Kong, S.P.; Lin, J. Salvianolic Acid B Reduces Oxidative Stress to Promote Hair-Growth in Mice, Human Hair Follicles and Dermal Papilla Cells. *Clin. Cosmet. Investig. Dermatol.* **2024**, *17*, 791–804. [CrossRef]
44. Gupta, A.; Venkataraman, M.; Talukder, M.; Bamimore, M. Finasteride for hair loss: A review. *J. Dermatol. Treat.* **2022**, *33*, 1938–1946. [CrossRef]
45. Arif, T.; Dorjay, K.; Adil, M.; Sami, M. Dutasteride in androgenetic alopecia: An update. *Curr. Clin. Pharmacol.* **2017**, *12*, 31–35. [CrossRef]
46. Carmeliet, P.; Jain, R.K. Molecular mechanisms and clinical applications of angiogenesis. *Nature* **2011**, *473*, 298–307. [CrossRef]